In-Plane Properties and Modeling of Reduced Beam Sections

PIERRE DUMONTEIL

In the seismic design of steel frames, one of the objectives is to provide ductile beams capable of energy dissipation through the formation of plastic hinges (or "fuses"). With wide-flange shapes, Iwankiw (1997) proposes to force these hinges away from the brittle zones near the column faces by reducing the beam section at some specified distance from these faces. Figure 1a shows how this is done by means of circular cuts in the flanges.

Obviously, the cuts change the overall elastic properties of the reduced beam sections (RBS). Iwankiw and Mohammadi (2004) describe one approach to evaluate the reduction in elastic stiffness. However, the cuts also affect the fixed-end actions used in the elastic analysis of the structure. Our first objective will be to compute not only the stiffness properties of RBS, but also the fixed-end actions.

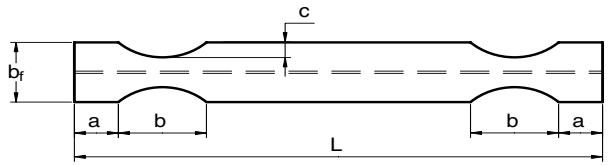

(a) Plan View of Flanges and Reducing Cuts

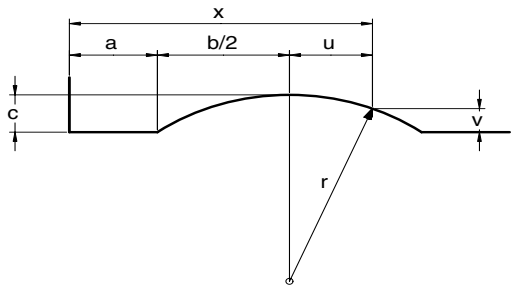

(b) Geometry of Cut

Fig. 1. Dimensions.

Pierre Dumonteil is a retired licensed professional engineer, Centennial, CO.

Most structural analysis programs found in design offices do not let the designer input stiffness matrices and fixed-end actions. Input of beam elements is usually limited to prismatic or tapered beams. Our second objective will be to show how this difficulty may be overcome by modeling a RBS with three prismatic beam elements of suitable properties.

Some very simple frames will be used as examples to compare interstory drifts and examine the Q_{33} method proposed by Iwankiw and Mohammadi. Coincidentally, these calculations lead to the observation that beam shear deformation is not always negligible.

REDUCED SECTION PROPERTIES

The geometry of the section-reducing cuts is shown on Figure 1b, using the notations of FEMA 350 (FEMA, 2000). Both flanges are cut in an identical manner, and the cuts are symmetrical about the midsection of the beam. Given the depth of the cuts c, and the chord b, the radius of the cut is then

$$r = \frac{b^2 + 4c^2}{8c} \tag{1}$$

At a distance $u = x - a - b/2$ from the axis of symmetry of the cut, the depth of cut is

$$v = \sqrt{r^2 - u^2} - r + c = \sqrt{r^2 - \left(x - a - \frac{b}{2}\right)^2} - r + c \tag{2}$$

The cuts reduce the moment of major inertia I_O of the original section (listed as I_x in the AISC manuals) by the amount

$$\Delta I(x) = I_O - I(x) = t_f \left[(d_b - t_f)^2 + \frac{t_f^2}{3} \right] v(x) \tag{3}$$

They also reduce the section area A by the amount

$$\Delta A(x) = 4\, t_f v(x) \tag{4}$$

The minimum plastic modulus Z_{RBS} occurs at the sections of deepest cut:

$$Z_{RBS} = Z - 2ct_f (d_b - t_f) \tag{5}$$

In this last expression, d_b denotes the depth of the beam.

ROTATIONAL FLEXIBILITY AND ROTATIONAL STIFFNESS

Since the rotational stiffness matrix is derived from the rotational flexibility matrix (Beaufait, Rowan, Hoadley, and Hackett, 1975), we start with the latter. The elements of the rotational flexibility matrix for a beam symmetrical about midspan are (see Appendix)

$$f_{11} = f_{22} = \int_0^{L/2} \left[1 - 2\frac{x}{L}\left(1 - \frac{x}{L}\right)\right] \frac{dx}{EI(x)} + f_S$$
$$f_{12} = f_{21} = -\int_0^{L/2} 2\frac{x}{L}\left(1 - \frac{x}{L}\right) \frac{dx}{EI(x)} + f_S \tag{6}$$

Omitting the shear term f_S for the time being, note that the moment of inertia is constant along the beam, except at the cuts. The flexibility element f_{11} may be written

$$f_{11} = \int_0^{L/2} \left[1 - 2\frac{x}{L}\left(1 - \frac{x}{L}\right)\right] \frac{dx}{EI_o} + \int_a^{a+b} \left[1 - 2\frac{x}{L}\left(1 - \frac{x}{L}\right)\right] \left(\frac{1}{EI(x)} - \frac{1}{EI_o}\right) dx \tag{7}$$

The first integral represents the flexibility element f_{11} for the original prismatic beam, that is, $f_{11} = L/(3EI_O)$. This yields for the RBS beam

$$f_{11} = \frac{L}{EI_o}\left\{\frac{1}{3} + \frac{1}{L}\int_a^{a+b} \left[1 - 2\frac{x}{L}\left(1 - \frac{x}{L}\right)\right]\left(\frac{I_o}{I(x)} - 1\right) dx\right\}$$
$$= \frac{L}{EI_o}\left\{\frac{1}{3} + \frac{1}{L}\int_a^{a+b} \left[1 - 2\frac{x}{L}\left(1 - \frac{x}{L}\right)\right]\frac{\Delta I(x)}{I_o - \Delta I(x)} dx\right\} \tag{8}$$

Equation 8 may be recast in dimensionless form

$$\varphi_{11} = \frac{EI_0}{L} f_{11} = \frac{1}{3} + T_1$$
$$\text{with } T_1 = \frac{1}{L}\int_a^{a+b} \left[1 - 2\frac{x}{L}\left(1 - \frac{x}{L}\right)\right] \frac{\Delta I(x)}{I_o - \Delta I(x)} dx \tag{9}$$

Developing f_{12} in a similar manner yields

$$\varphi_{12} = \frac{EI_0}{L} f_{12} = -\frac{1}{6} - T_2$$
$$\text{with } T_2 = \frac{1}{L}\int_a^{a+b} 2\frac{x}{L}\left(1 - \frac{x}{L}\right) \frac{\Delta I(x)}{I_o - \Delta I(x)} dx \tag{10}$$

Closed-form expressions of these definite integrals are possible (Chambers, Almudhafar, and Stenger, 2003), but at the cost of calculations so formidable that one must agree with Iwankiw and Mohammadi that numerical integration is the only practical approach. The two definite integrals T_1 and T_2 are of the form

$$T = \int_a^{a+b} g(x)\, dx \tag{11}$$

Applying Simpson's rule over the five points of Figure 2 gives the approximate value

$$T \cong \frac{1}{3}\left(\frac{b}{4}\right)\left(g_0 + 4g_1 + 2g_2 + 4g_3 + g_4\right) \tag{12}$$

In this equation, g_0, g_1, g_2, g_3, and g_4 are the values assumed by the function $g(x)$ at the integration points 0, 1, 2, 3, and 4. Since $\Delta I = 0$ at points 0 and 4, $g_0 = g_4 = 0$, and the result is simply

$$T \cong \frac{b}{6}\left(2g_1 + g_2 + 2g_3\right) \tag{13}$$

(Using the nondimensional flexibilities, φ provides a check on the computations since φ_{11} and φ_{12} must be numerically larger than ⅓ and ⅙, respectively, but by not more than about 20%).

At this stage, the shear flexibility may be added to obtain the full flexibility elements:

$$\begin{Bmatrix} f_{11} \\ f_{12} \end{Bmatrix} = \frac{L}{EI_o}\begin{Bmatrix} \varphi_{11} + \varphi_s \\ \varphi_{11} + \varphi_s \end{Bmatrix}$$
$$\text{with } \varphi_s = \frac{EI_0}{L} f_s = \frac{EI_o}{GA_s L^2} \tag{14}$$

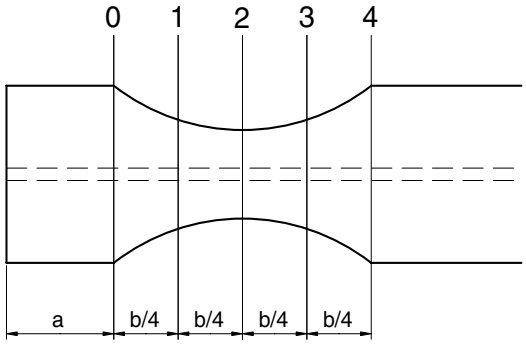

Fig. 2. Integration points.

The rotational stiffness elements k_{11} and k_{12} are then

$$k_{11} = \frac{f_{11}}{f_{11}^2 - f_{12}^2};\ k_{12} = -\frac{f_{12}}{f_{11}^2 - f_{12}^2} \tag{15}$$

The cuts also increase the magnitude of the extensional flexibility f_{ax}:

$$f_{ax} = \frac{L}{EA}\varphi_{ax} = \frac{L}{EA}\left(1 + \frac{1}{L}\int_a^{a+b} \frac{2\Delta A}{A - \Delta A}dx\right) \tag{16}$$

This equation, which takes advantage of symmetry, is treated in the same fashion as Equations 9 and 10. The corresponding stiffness elements are numerically equal to the reciprocal of f_{ax}.

Regarding the accuracy of the results, note that the integrands of Equations 9 and 10 are suitable for Romberg integration, which yields numerically exact results. Compared with the Romberg results, the parabolic rule of Equation 13 is found to give an accuracy of better than 0.2% for T_1 and T_2. Since these two factors represent corrections never amounting to more than 20% of the total, the overall error of the simple parabolic rule is less than 0.2 × 0.2% = 0.04%, or about one unit in the fourth significant digit.

Consider the W24×76 beam used as an example by Chambers et al. (2003) and Iwankiw and Mohammadi (2004). With a span of 18 ft, its span-to-depth ratio is 9 to 1. The dimensions of the cuts are a = 5.00 in., s = 20 in., and c = 2.00 in. This cut (c/b_f = 0.222) reduces the plastic section modulus by 31.6%. The relative rotational flexibility φ_{11} increases from ⅓ = 0.3333 to 0.3599 (+8.0%), while $|\phi_{12}|$ goes up from ⅙ = 0.1667 to 0.1706 (+2.3%). The decrease in stiffness is more pronounced than the increase in flexibility. Using Iwankiw and Mohammadi's notation, the "cut to uncut" reduction factors are Q_{11} = 0.896 for k_{11} and Q_{12} = 0.849 for k_{12}. Since $k_{11} = k_{22}$, all other elements of the stiffness matrix are proportional to $k_{33} = (k_{11} + k_{12})/L$, for which the reduction factor is Q_{33} = 0.880. These results agree with those of Chambers et al. (2003) and Iwankiw and Mohammadi (2004). The extensional flexibility φ_{ax} goes up by 2.3%, so that the extensional stiffness decreases by 2.3%. However, the extensional flexibility of the beams is unlikely to be of importance in moment frames.

SHEAR DEFORMATION

If shear deformation is included in both uncut and RBS beams, the decreases are slightly less pronounced, but not significantly so: k_{11} decreases by 9.3% (Q_{11} = 0.907), k_{12} by 13.7% (Q_{12} = 0.863), while $k_{11} + k_{12}$ decreases by 10.7% (Q_{33} = 0.893). However, these figures mask the fact that shear may have a rather large effect on the rotational stiffness elements. The shear area is $A_S = t_w(d_b - t_f)$ = (0.440)(23.9 – 0.680) = 10.2 in.^{2}, so that the nondimensional shear flexibility is φ_S = 0.01141. For the uncut prismatic beam, shear causes k_{11} to decrease by 9.0%, k_{12} by 18.1%, and $k_{11} + k_{12}$ by 12.0%. For the RBS beam, shear reduces k_{11} by 7.9%, k_{12} by 16.7%, and $k_{11} + k_{12}$ by 10.8%.

FIXED-END ACTIONS

With a uniform load w, the calculations of the Appendix give

$$\omega_2 = -\omega_1 = -\frac{\varphi_{12}}{4}\frac{wL^3}{EI_O} \tag{17}$$

For the W24×76 with a span of 18 ft used as an example, there is a small numerical increase of φ_{12} (2.3%), but there is a larger decrease in stiffness since the multiplier $k_{11} - k_{12}$ decreases by 5.7%. Thus, the fixed-end moments experience a numerical decrease of 3.5%. For the same example, the magnitude of the fixed-end moments decreases by 4.2% for a centrally applied vertical load, 4.0% for two equal loads applied at the third points, and 3.8% for three equal loads applied at the quarter points.

FINITE SIZE OF CONNECTIONS

The strong-axis connections investigated by Jones, Fry, and Engelhardt (2002) have an offset of about 9 in., with the cuts starting 9 in. from the column faces, or 9 + 9 = 18 in. from their centerlines. This offset has the same magnitude as the start of the cuts (dimension a of Figure 1). For the weak-axis connections tested by Gilton and Uang (2002), the plates attaching the beam flanges to the column web project 3 in. beyond the column flanges, and the cut, which starts 9 in. from the end of the beam proper, actually starts 20.3 in. from the centerline of the column. Obviously, these offsets must be included in our calculations.

Section 3.5.5 of FEMA 350 (FEMA, 2000), "Reduced Beam Section Connections," limits the depth range of the columns in special moment frames to the W12 and W14 shapes (there is no depth limitation for ordinary moment frames). It also specifies

$$a \cong (0.5 \text{ to } 0.75)b_f \tag{18a}$$

$$b \cong (0.65 \text{ to } 0.85)\ d_b \tag{18b}$$

$$c \le 0.25b_f \tag{18c}$$

Note that a is always measured from the face of the column (d_b is the depth and b_f is the flange width of the beam). Assume that the W24×76 of the example is connected to W12 columns. For a strong-axis connection, the face of the column would be about 6 in. from the column centerline, and

the start of the cut would be approximately 11 in. from the column centerline. Except for very rigid panel zones, which would be modeled as rigid offsets, standard software does not allow for easy modeling of panel zones. Section 2.8.2.3 of FEMA 350, "Connection Stiffness," "recommends use of a simpler approach, in which panel zones are neglected in the model and center-line-to-center-line framing dimensions are used."

To account for the column depth d_c, dimension a is simply replaced with $a' = a + d_c/2$. For the W24×76 of the example, moving the cuts 6 in. away from the beam ends stiffens the RBS beam slightly, since k_{11} increases by 1.0% and k_{12} by 2.3%. These figures include the effect of shear, but the increases are very similar if shear is neglected.

MODELING OF REDUCED BEAM SECTION

Since most structural analysis programs usually restrict the input of beam elements to prismatic or tapered beams, an artifice must be found in modeling the RBS beam. Suppose that, instead of a single beam, we input three prismatic beam elements as shown on Figure 3, with moments of inertia I_O/α and I_O/β; this makes available two parameters α and β, which may be adjusted to provide a suitable approximation.

Consider the beam consisting of the three segments of Figure 3. It is symmetrical about the center of the span, and therefore its rotational flexibilities may be computed by means of Equation A9 of the Appendix. In nondimensional form, we find

$$\begin{aligned}\varphi_{11} &= \frac{\alpha}{L}\int_0^{L/4}\left[1-2\frac{x}{L}\left(1-\frac{x}{L}\right)\right]dx \\ &\quad +\frac{\beta}{L}\int_{L/4}^{L/2}\left[1-2\frac{x}{L}\left(1-\frac{x}{L}\right)\right]dx = \frac{19\alpha+13\beta}{96} \\ \varphi_{12} &= -\frac{\alpha}{L}\int_0^{L/4}2\frac{x}{L}\left(1-\frac{x}{L}\right)dx \\ &\quad -\frac{\beta}{L}\int_{L/4}^{L/2}2\frac{x}{L}\left(1-\frac{x}{L}\right)dx = -\frac{5\alpha+11\beta}{96}\end{aligned} \tag{19}$$

Solving for α and β, we have

$$\begin{aligned}\alpha &= \frac{2}{3}(11\varphi_{11}+13\varphi_{12}) \\ \beta &= -\frac{2}{3}(5\varphi_{11}+19\varphi_{12})\end{aligned} \tag{20}$$

For the W24×76 of the example, we find $\alpha = 1.161$ and $\beta = 0.961$. Accordingly, the RBS may be modeled with two outer segments with $I = 2{,}100/1.161 = 1{,}809$ in.^{4} and a central segment with $I = 2{,}100/0.961 = 2{,}185$ in.^{4} Each segment is given a shear area $A_S = 10.2$ in.^{2} To have the same axial stiffness, all three segments are given a section area equal to the uncut area divided by the relative flexibility φ_{ax}, that is, $A = 22.4/1.023 = 21.9$ in.^{2} These steps ensure that the three-element model will have the same k_{11} and k_{12}, and therefore the same stiffness matrix, as the RBS beam.

Since we have forced the flexibilities and stiffnesses of the model to equal those of the RBS beam, an immediate consequence of Equation A12 of the Appendix is that the fixed-end moments caused by a uniform load w are identical in the RBS beam and the segmented model. In the case of a centrally applied concentrated load P, the end rotation is, in nondimensional form,

$$\omega^* = \frac{EI}{PL^2}\omega_2 = \frac{\alpha+3\beta}{64} = -\frac{\varphi_{11}+11\varphi_{12}}{24} \tag{21}$$

For the W24×76 of the example, Equation 21 gives $\omega^* = 0.0633$ instead of $\omega^* = 0.0636$, the value obtained by numerical integration. Two equal loads applied at the third points give $\omega^* = 0.1131$, in comparison with $\omega^* = 0.1132$ by numerical integration. Finally, for three equal loads applied at the quarter points, we arrive at $\omega^* = 0.1595$ compared with $\omega^* = 0.1593$ by numerical integration.

Since the end rotations, and therefore the fixed-end actions, obtained with the model are accurate, the practical consequence is that we need to compute only the flexibilities φ_{11}, φ_{12}, and φ_{ax}, and the two parameters α and β. This computation is easily set up on a spreadsheet. The fixed-end actions need not be considered, since they will be adequately taken care of by the structural analysis program.

EXAMPLES

To get at least some orders of magnitude on the influence of RBS beams, the rigid frames of Figure 4 will serve as examples, albeit rather simplistic ones. For the single-

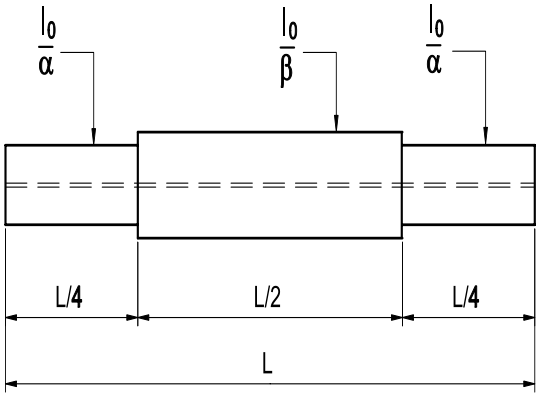

Fig. 3. Three-segment model.

Table 1. W-Shapes and Cuts Used in the Examples							
Example	Frame (Fig. 4)	Shape	Span L, ft	Column d_c, in.	Dimensions of cuts		
					a, in.	b, in.	c, in.
I	4 a	W24×76	18	12	6	18	2.25
II	4 b	W36×256	22	14	8	28	3
III	4 c	W30×132	30	12	7	22	2.625
IV	4 c	W30×173	24	12	10	22	3.75

story building of Figure 4a, the drift is not expected to be a determining factor in the design, assuming that a moment frame would be justified for this application. Figure 4b schematizes frames used for process towers, which often require open framing to allow passage of conveyors or access to large equipment. A simple building frame is sketched in Figure 4c.

The examples use a story height H = 12 ft. An important variable is the ratio $(I/L)_c$ of the columns, for which a value $(I/L)_c = (I/L)_b = I_0/L$ is considered somewhat representative. Decreasing the $(I/L)_c$ of the columns decreases the relative interstory drift of the RBS frames compared with the uncut frames. Table 1 shows the dimensions a and b, chosen near the middle of the ranges allowed by FEMA (2000), Section 3.5.5.1, and the cut c set close to its allowable maximum 0.25 b_f specified in the same Section. Two load cases are considered: (1) a uniform vertical load on all floors, and (2) horizontal seismic forces, applied at each floor, and increasing in arithmetic progression (1, 2, 3, …) from bottom to top floor.

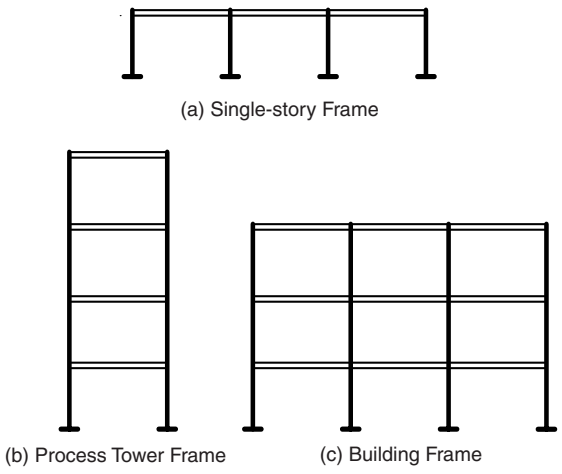

Fig. 4. Frame examples.

Even though the maximum cuts in the W24×76 beams of the frame in Figure 4a reduce their bending stiffness by 10% or more (Q_{33} = 0.887), the moments at the column faces due to the vertical loads in the RBS beams are reduced by about 4% compared with the uncut beams. It would be acceptable to neglect the reduction in stiffness to determine the forces in the column/beam connections. As expected, the interstory drift increase is small, only 2.6%.

In Example II, using the frame in Figure 4b, the moments at the column faces undergo minimal changes, less than 3%, between uncut and RBS frames. The drift of the top story is increased by 10.6% if shear is neglected and 9.3% otherwise.

For Example III, using the frame in Figure 4c (W30×132), RBS beams decrease the moments at the column faces by 4% or less. The interstory drift increases by 5.9% if shear is neglected and 5.7% otherwise. With the heavier, stockier beams of Example IV (W30×173), RBS beams increase the interstory drift by 7.3% without shear and 6.7% with shear.

Iwankiw and Mohammadi's Q_{33} Method

Iwankiw and Mohammadi suggest the simple approach to replace the RBS beam with a prismatic one having a reduced moment of inertia $I_R = Q_{33}\ I_0$. They do not consider shear, but, if the software allows, shear may be included by giving a shear area A_S to the substitute beam. Because the computa-

tions are so easily set up in a spreadsheet, the Q_{33} values used here are calculated directly from the section properties of the W-shapes, rather than with the regression formula established by Iwankiw and Mohammadi. With this stipulation, it was found that, in general, the Q_{33} multiplier method (Q_{33} method in short) gives accurate estimates of the interstory drift.

Shear Deformation and Interstory Drift

Finally, consider the influence of shear on interstory drift. For Example I (Frame 4a), shear deformation adds only 2.7% to the drift. In Example II (Frame 4b), shear increases the drift of the uncut frame by 15.2% and that of the RBS frame by 13.9%. In Example III (Frame 4c), shear alone increases the top story drift in the uncut frame by 4.2% and by 4.0% in the RBS frame. In Example IV (Frame 4c), including shear adds 8.8% to the top story drift in the uncut frame and 8.2% in the RBS frame. While Example II may be somewhat extreme, Example IV shows that there are cases in which the influence of shear may not be small.

Some commercially available analysis programs do not consider shear at all, which is regrettable. Other matrix analysis packages usually require some care to input a meaningful shear area. Omitting shear deformation leads to discrepancies when calculations based on the engineering beam theory are compared with the results of finite element analyses employing plates to model structural shapes. While including shear deformation is certainly a complication in hand calculations, it is only a very minor one in computer-based analyses.

FEMA 350 does not mention whether shear deformation is to be included in the elastic analysis model. The AISC *Seismic Provisions for Structural Steel Buildings* (AISC, 2002), Section C5 of the Commentary, state that "the analytical model used to estimate building drift should accurately account for the stiffness of the frame elements and connections …" It would seem that, for the sake of accuracy, shear deformation of the beams should be included in the elastic model, since it contributes significantly to the sidesway.

CONCLUSION

It has been shown how, using the exact formulation of flexibilities for nonprismatic beams, a simple scheme of numerical integration over three points in the cut area allows a quick and accurate calculation of the rotational and axial flexibilities of a RBS beam. With appropriate modifications of the numerical integration scheme, other types of reinforcements or reductions can easily be calculated.

The stiffness matrix of the RBS beam could be determined from these flexibilities, but this knowledge is not helpful since many structural analysis programs do not allow its input. To get around this difficulty, it is proposed to replace the RBS with three prismatic beam elements, whose properties are determined so that the assembly of these elements has the same flexibilities as the original RBS.

Some simple examples have been given to provide some orders of magnitude and compare the results with those of the Q_{33} method proposed by Iwankiw and Mohammadi. This method gives excellent estimates of the drift. However, these results also show that shear deformation, especially with beams of small span-to-depth ratios, can increase very substantially the estimated drift. In the author's opinion, accounting for beam shear deformation is a simple task with a computer and it should be automatically included in matrix structural analyses, especially those involving sidesway or drift.

REFERENCES

AISC (2002), *Seismic Provisions for Structural Steel Buildings*, ANSI/AISC 341, American Institute of Steel Construction, Inc., Chicago, IL, May 21.

Beaufait, F.W., Rowan W.H., Hoadley, P.G., and Hackett, R.M. (1975), *Computer Methods of Structural Analysis*, Vanderbilt University.

Chambers, J.J., Almudhafar, S., and Stenger, F. (2003), "Effect of Reduced Beam Section Frame Elements on Stiffness of Moment Frames," *Journal of Structural Engineering*, ASCE, Vol. 129, No. 3, pp. 383–393.

FEMA (2000), *Recommended Seismic Design Criteria for New Steel Moment-Frame Buildings*, FEMA 350, Federal Emergency Management Administration, Washington, DC, June.

Gilton, C.S., and Uang, C.-M. (2002), "Cyclic Response and Design Recommendations of Weak-Axis Reduced Beam Section Moment Connections," *Journal of Structural Engineering*, ASCE, Vol. 128, No. 4, pp. 452–463.

Iwankiw, N.R. (1997), "Ultimate Strength Considerations for Seismic Design of the Reduced Beam Section (Internal Plastic Hinge)," *Engineering Journal*, AISC, 1st Quarter, pp. 3–16.

Iwankiw, N.R., and Mohammadi, J. (2004), "Elastic In-Plane Stiffness for a Circular Cut Reduced Beam Section (RBS)," *Engineering Journal*, AISC, 1st Quarter, pp. 23–36.

Jones, S.L., Fry, G.T, and Engelhardt, M.D. (2002), "Experimental Evaluation of Cyclically Loaded Reduced Beam Section Connections," *Journal of Structural Engineering*, ASCE, Vol. 128, No. 4, pp. 441–451.

Weaver, Jr., W., and Gere, J.M. (1980), *Matrix Analysis of Framed Structures*, Van Nostrand Rheinhold Co., New York, NY.

APPENDIX
ROTATIONAL FLEXIBILITY AND STIFFNESS EQUATIONS

Since the rotational stiffness matrix is derived from the rotational flexibility matrix, we start with the latter. The bending moment in the beam is

$$M(x) = -\left(1-\frac{x}{L}\right)M_1 + \left(\frac{x}{L}\right)M_2 + m(x) \qquad \text{(A1)}$$

M_1 and M_2 are the end moments and $m(x)$ is the bending moment in a simple beam of span L under the same actions. The complementary energy of the beam is

$$U^* = \frac{1}{2}\int_0^L \frac{\left[M(x)\right]^2}{EI(x)}dx + \frac{1}{2}\int_0^L \frac{\left[V(x)\right]^2}{GA_S(x)}dx \qquad \text{(A2)}$$

Apply Castigliano's second theorem to obtain

$$\begin{aligned}\theta_1 &= \frac{\partial U^*}{\partial M_1} = f_{11}M_1 + f_{12}M_2 + \omega_1 \\ \theta_2 &= \frac{\partial U^*}{\partial M_2} = f_{21}M_1 + f_{22}M_2 + \omega_2\end{aligned} \qquad \text{(A3)}$$

The elements of the flexibility matrix are

$$\begin{aligned}f_{11} &= \int_0^L \left(1-\frac{x}{L}\right)^2 \frac{dx}{EI(x)} + \frac{1}{L^2}\int_0^L \frac{dx}{GA_S(x)} \\ f_{12} = f_{21} &= -\int_0^L \frac{x}{L}\left(1-\frac{x}{L}\right)\frac{dx}{EI(x)} + \frac{1}{L^2}\int_0^L \frac{dx}{GA_S(x)} \\ f_{22} &= \int_0^L \left(\frac{x}{L}\right)^2 \frac{dx}{EI(x)} + \frac{1}{L^2}\int_0^L \frac{dx}{GA_S(x)}\end{aligned} \qquad \text{(A4)}$$

The rotational stiffness matrix is the inverse of the flexibility matrix (Beaufait et al., 1970)

$$\mathbf{k} = \begin{bmatrix}k_{11} & k_{12} \\ k_{21} & k_{22}\end{bmatrix} = \mathbf{f}^{-1} = \begin{bmatrix}f_{11} & f_{12} \\ f_{21} & f_{22}\end{bmatrix}^{-1} \qquad \text{(A5)}$$

The end rotations ω_1 and ω_2 of the simple beam are

$$\begin{aligned}\omega_1 &= -\int_0^L \left(1-\frac{x}{L}\right)\frac{m(x)\,dx}{EI(x)} + \frac{1}{L}\int_0^L \frac{t(x)\,dx}{GA_s(x)} \\ \omega_2 &= \int_0^L \left(\frac{x}{L}\right)\frac{m(x)\,dx}{EI(x)} + \frac{1}{L}\int_0^L \frac{t(x)\,dx}{GA_s(x)}\end{aligned} \qquad \text{(A6)}$$

where $t(x) = dm/dx$ is the corresponding shear. The fixed end moments FM_1 and FM_2 are then

$$\begin{Bmatrix}FM_1 \\ FM_2\end{Bmatrix} = -\left[\mathbf{k}\right]\begin{Bmatrix}\omega_1 \\ \omega_2\end{Bmatrix} = -\begin{Bmatrix}k_{11}\,\omega_1 + k_{12}\,\omega_2 \\ k_{21}\,\omega_1 + k_{22}\,\omega_2\end{Bmatrix} \qquad \text{(A7)}$$

These equations are valid for any beam, prismatic or not. We turn now to specializing them for our specific purpose.

Shear energy considerations show that, for a W-shape, the flange cuts have a negligible influence on the shear area, which may be considered constant. Moreover, the best approximation is $A_S = t_w(d_b - t_f)$, except for very heavy sections used essentially as columns. This rejoins Weaver and Gere's recommendation (1980). The flexibility f_S is then

$$f_S = \frac{L}{GA_S} = \frac{L}{G\,t_w(d_b - t_f)} \qquad \text{(A8)}$$

Since f_S is only a corrective term, using $A_S \cong A_w = d_b\,t_w$ would be acceptable, except again for heavy W-shapes.

Symmetry allows the specialization of Equation A4

$$\begin{aligned}f_{11} = f_{22} &= \frac{f_{11} + f_{22}}{2} \\ &= \int_0^{L/2} \left[1 - 2\frac{x}{L}\left(1-\frac{x}{L}\right)\right]\frac{dx}{EI(x)} + f_S \\ f_{12} = f_{21} &= -\int_0^{L/2} 2\frac{x}{L}\left(1-\frac{x}{L}\right)\frac{dx}{EI(x)} + f_S\end{aligned} \qquad \text{(A9)}$$

If A_S is constant, the integrals containing $t(x)$ in Equation A6 evaluate to zero. This is also true if the loading is symmetrical, since the shear $t(x)$ is then antisymmetrical, Further, with symmetrical loads, the rotations ω_1 and ω_2 are equal in magnitude, so that

$$\omega_2 = -\omega_1 = \frac{\omega_2 - \omega_1}{2} = \int_0^{L/2} \frac{m(x)}{EI(x)}dx \qquad \text{(A10)}$$

The fixed-end moments take the simple form

$$FM_1 = -FM_2 = (k_{11} - k_{12})\omega_2 \qquad \text{(A11)}$$

It is easily found that the terms containing f_S in $k_{11} - k_{12}$ cancel out since the beam is assumed symmetrical. Therefore, the shear has no effect on the fixed-end moments.

Applying Equation A10 to the case of a uniform load w, we find the convenient result:

$$\omega_2 = \left(\frac{wL^2}{2}\right)\int_0^{L/2} \frac{x}{L}\left(1-\frac{x}{L}\right)\frac{dx}{EI(x)} = -\frac{wL^3}{4EI_0}\,\varphi_{12} \qquad \text{(A12)}$$

In other cases, the evaluation of ω_2 requires numerical integration.